Hindawi Publishing Corporation
Journal of Nanomaterials
Volume 2015, Article ID 130270, 12 pages
http://dx.doi.org/10.1155/2015/130270

Research Article

Wettability Investigation of UV/O_3 and Acid Functionalized MWCNT and MWCNT/PMMA Nanocomposites by Contact Angle Measurement

Seil Kim,[1] Abdullah A. Kafi,[2] Ehsan Bafekpour,[3] Young-In Lee,[4] Bronwyn Fox,[5] Manwar Hussain,[1] and Yong-Ho Choa[1]

[1]*Department of Fusion Chemical Engineering, Hanyang University, Ansan 426-791, Republic of Korea*
[2]*Sabic SPADC, Riyadh Techno-Valley, Riyadh 11195, Saudi Arabia*
[3]*Department of Materials Engineering, Monash University, Clayton, VIC 3800, Australia*
[4]*Department of Materials Science and Engineering, Seoul National University of Science & Technology, Seoul 139-743, Republic of Korea*
[5]*Institute for Frontier Materials, Deakin University, Geelong, VIC 3220, Australia*

Correspondence should be addressed to Manwar Hussain; manwarh@hanyang.ac.kr and Yong-Ho Choa; choa15@hanyang.ac.kr

Received 20 November 2014; Revised 17 December 2014; Accepted 17 December 2014

Academic Editor: Yingkui Yang

The dispersion state of individual MWCNT in the polymer matrix influences the mechanical, thermal, and electrical properties of the resulting composite. One method of obtaining a good dispersion state of MWCNT in a polymer matrix is to functionalize the surface of MWCNT using various treatments to enhance the surface energy and increase the dispersibility of MWCNT. In this study, wettability and surface energy of UV/O_3 and acid-treated multiwall carbon nanotubes (MWCNTs) and its polymethyl methacrylate (PMMA) polymer nanocomposites were measured using contact angle analysis in various solvent media. Contact angle analysis was based on ethylene glycol-water-glycerol probe liquid set and data was further fitted into geometric mean (Fowkes), van Oss-Chaudhury-Good (GvOC), and Chang-Qing-Chen (CQC) models to determine both nonpolar and acid base surface energy components. Analysis was conducted on MWCNT thin films subjected to different levels of UV/O_3 and acid treatments as well as their resulting MWCNT/PMMA nanocomposites. Contact angle analysis of thin films and nanocomposites revealed that the total surface energy of all samples was well fitted with each other. In addition, CQC model was able to determine the surface nature and polarity of MWCNT and its nanocomposites. Results indicated that the wettability changes in the thin film and its nanocomposites are due to the change in surface chemistry. Finally, electrical properties of nanocomposites were measured to investigate the effect of surface functionality (acid or basic) on the MWCNT surfaces.

1. Introduction

Numerous polymer composites' fabrication has been focused to improve the electrical and mechanical properties for various applications [1, 2]. Many types of polymer matrix such as polystyrene (PS), polyethylene (PE), polyvinyl acetate (PVAc), and poly(methyl methacrylate) (PMMA) have been used to synthesize the polymer composite until now. Among the polymers, PMMA is the most widely studied polymer as a matrix due to its low cost, high optical loss in the visible spectrum, stability, high scratch hardness, and low glass transition temperature [3]. Above all, PMMA is one of the polymers that are most resistant to sunshine exposure, as well as the presence of ozone. These properties of PMMA make it a suitable product intended for long open-air operation.

A large number of composite researches have been performed with PMMA matrix and inorganic materials such as carbon nanotubes (CNTs) [4, 5], carbon black [6, 7], and graphene [8, 9]. Amongst all, CNTs are regarded as promising candidate for electrical and mechanical reinforcement of polymers. Composites reinforced with CNTs exhibited unique physical, mechanical, and electrical properties derived from high specific surface area, high aspect ratio, and superior conductivity of CNTs [10]. The dispersibility of CNT

in various solvents has been studied extensively in recent years. Researchers are mainly trying to achieve good dispersibility using surface treatment or functionalization using polar groups such as carbonyl (–C(O)–), carboxyl (–COOH), and hydroxyl (–OH), which assist in their solubility in polar solvents. Philip et al. [11] designed MWCNT/PMMA composite thin films to study the effect of polar groups in MWCNT for a variety of gas sensing systems. Abraham et al. [12] designed a compact wireless gas sensor using a MWCNT/PMMA thin film chemiresistor with surface-treated MWCNTs to obtain better dispersion in the polymer matrix. Here, the dispersibility of MWCNT into polymer matrix always remains a challenge. For all of the above-mentioned applications, effective dispersion, and interfacial bonding to polymers, surface functionalization of MWCNT is extremely necessary [13–15]. In this research we analysed surface energy through contact angle measurement which provided valuable chemical and physical aspects of CNT surfaces. In addition, the surface energy is an important parameter in understanding the wetting of a material in addition to adhesion and dispersion properties or compatibility with a solvent or polymer [16]. It can be measured by several established approaches [17].

Contact angle measurement is a simple method to determine the surface energy which considers the behaviour between the liquid and solid under contact and the formation of droplets on a thin film. When a liquid drop beads up and produces a large contact angle, the surface energy is relatively low and adhesion is poor. The methods used to determine the surface energy components require measuring the contact angles of a variety of liquids with known polar and dispersion components of the total surface tension. Commonly, a successfully modified surface will exhibit a lower contact angle and higher surface energy [18]. The acid-base component of the surface energy is generally estimated using contact angle measurements followed by calculations using a range of statistical thermodynamic models. There are many techniques available to determine the surface energy from contact angle values. Amongst many, an established approach to examine surface energy of various materials was proposed by van Oss et al. [19], here referred to as the van Oss-Chaudhury-Good (GvOC) model, in which specific acid and base parameters of the surface free energy of a substance are determined based on contact angle analysis. However, the conventional calculation for the GvOC model does not allow for the negative acid and base parameter which leads to misleading information about surface. Similarly, Chen and Chang [20] proposed a semiempirical acid-based approach, here referred to as the Chang-Qin-Chen (CQC) model, to overcome the present drawbacks of the GvOC model. The Chang model is more robust than the GvOC model as it can measure both attractive and repulsive characters of acid-base interactions. In this research, we synthesized the MWCNT thin film and the MWCNT/PMMA composite with functionalized MWCNT, treated by UV/O_3 and acid and calculated the surface energy using contact angle measurement, which was fitted from above various models. We further studied correlation between surface energy, dispersibility, and electrical properties in polymer matrix by measuring the sheet resistance of the pristine MWCNT, UV/O_3 MWCNT, and acid MWCNT/PMMA composite.

2. Experimental

2.1. Materials. The MWCNTs were synthesized by thermal chemical vapour deposition and supplied by Hanwa Nanotech Co. Ltd., Korea. The carbon purity and apparent density of the MWCNTs were about 95 wt% and 0.1 g/cm^3, respectively. The specific surface area and aspect ratio were ~225 m^2/g and ~10^5, respectively. Poly(methyl methacrylate) (PMMA) with an average molecular weight of 120,000 g/mol was purchased from Sigma-Aldrich.

2.2. Fabrication of Pretreated MWCNTs and MWCNT/PMMA Nanocomposites. Pretreatment of the MWCNTs was performed by UV/O_3 and acid treatment. The MWCNT treatment methods and fabrication of MWCNT/PMMA nanocomposites were presented in our previous study [21]. The MWCNTs were treated with UV/O_3 for 30, 60, and 120 min using a UV/O_3 generator (Model number 42, Jelight, Co.). High concentration acid treatment of the MWCNTs was performed using a mixture of sulphuric and nitric acids for 6, 12, and 24 hours. MWCNT/PMMA nanocomposites containing 3 wt% MWCNTs were synthesized by a typical solution casting process. Characteristics of these two types of MWCNTs, UV/O_3- and acid-treated samples, were evaluated with various analysis tools.

2.3. Characterization

2.3.1. Contact Angle Measurement. Advancing contact angles were measured on the pristine-treated MWCNT thin films and their resulting MWCNT/PMMA nanocomposites using a contact angle measurement system (KSV Instruments Ltd., Finland) attached to a CAM101 video camera. Before the test, a 3 mL plastic syringe was cut at the very end of the tip using a precision cutter to slow down the motion of the probe liquids. Water (W), glycerol (G), and ethylene glycol (EG) were employed as the probe liquids where their nonpolar and polar surface energy components were obtained from the literature. The contact angle measurement was performed by placing a droplet of a probe liquid at various spots on the film's surface and recording images at a speed of 220 frames/sec. The contact angles were measured on three different places of both the MWCNT films and MWCNT/PMMA nanocomposites.

2.3.2. Determination of the Surface Energy. The surface free energy components were calculated from the contact angles measured using the water, ethylene glycol, and glycerol probe liquids according to the van Oss-Chaudhury-Good (vOCG) technique previously described in the literature [22]. The speciality of the vOCG method is that electron-acceptor (γ^+) and electron-donor (γ^-) surface energy parameters are used to describe acid-base interactions. The values of ${\gamma_S}^+$ and ${\gamma_S}^-$ for solids thin films and nanocomposites were determined using (1) applying multiple regression analysis where ${\gamma_S}^{LW}$ is

the dispersion component of the surface energy of the solid once contact angle, θ, is measured and applied as $\cos\theta$. Surface energy values for probe liquids represented as γ_{LV} (total), ${\gamma_L}^-$ (basic), and ${\gamma_L}^+$ (acidic) were taken from the literature:

$$\gamma_{LV}(1+\cos\theta) = 2\left[\sqrt{{\gamma_L}^{LW}{\gamma_S}^{LW}} + \sqrt{({\gamma_S}^+{\gamma_L}^-)} + \sqrt{({\gamma_L}^+{\gamma_S}^-)}\right]. \quad (1)$$

The acid-base components, ${\gamma_S}^{AB}$, and the total surface energy, ${\gamma_S}^{Total}$, of solids were calculated using the following equations:

$$\begin{aligned} {\gamma_S}^{AB} &= 2\sqrt{({\gamma_S}^+{\gamma_L}^-)}, \\ {\gamma_S}^{Total} &= {\gamma_S}^{LW} + {\gamma_S}^{AB}. \end{aligned} \quad (2)$$

For simplicity, the surface energy values are denoted as Gamma^T, Gamma^D, and Gamma^P throughout this paper.

Geometric Mean or Fowkes Approach. Good-Girifalco-Fowkes proposed [17, 23] that intermolecular forces resulted from both dispersive and polar interactions. Owens and Wendt [24] extended Fowkes' approach by grouping the nondispersive term into a polar contribution [25]. It is regarded as a breakthrough in understanding of wetting phenomena especially for nonpolar interactions between solid and liquid; it can be expressed as follows:

$${W_a}^{LW} = 2\sqrt{({\gamma_L}^{LW}{\gamma_S}^{LW})}, \quad (3)$$

where

$${\gamma_S}^{LW} = \frac{1}{4}{\gamma_L}^{\text{apolar}}\left(1+\cos\theta^{\text{apolar}}\right)^2, \quad (4)$$

$$W_a = \gamma_L(1+\cos\theta) = 2\left[\sqrt{({\gamma_L}^d{\gamma_S}^d)} + \sqrt{({\gamma_L}^p{\gamma_S}^p)}\right], \quad (5)$$

where ${\gamma_L}^d$ and ${\gamma_L}^p$ are the dispersion and polar components of the surface energy of liquid whereas ${\gamma_S}^d$ and ${\gamma_S}^p$ are the nonpolar and polar components of the surface energy of solid.

The van Oss-Chaudhury-Good (GvOC) Approach. van Oss and coworkers [26] proposed a generalized overview of the Fowkes geometric mean approach which explained that acid-base interaction was mainly based on two independent variables, namely, electron-acceptor (γ^+) and electron-donor (γ^-) surface energy parameters. van Oss et al. [26] modified (5) and inserted Lewis acid (+) and Lewis base (−) parameters instead of polar and dispersion surface energy components and thus the acid-base component of the work of adhesion across a solid-liquid interface could be expressed as follows:

$${W_a}^{AB} = 2\left[\sqrt{({\gamma_S}^+{\gamma_L}^-)} + \sqrt{({\gamma_L}^+{\gamma_S}^-)}\right]. \quad (6)$$

Now a combined equation can be obtained following $W_a = {W_a}^{LW} + {W_a}^{AB}$, where the values of W_a, ${W_a}^{LW}$, and ${W_a}^{AB}$ are incorporated from equations 5.4, 5.5, and 5.8:

$$\gamma_{LV}(1+\cos\theta) = 2\left[\sqrt{{\gamma_L}^{LW}{\gamma_S}^{LW}} + \sqrt{({\gamma_S}^+{\gamma_L}^-)} + \sqrt{({\gamma_L}^+{\gamma_S}^-)}\right]. \quad (7)$$

Equation (7) is called vOCG equation where ${\gamma_S}^{LW}$ is the dispersion component of the surface energy of solid. When ${\gamma_S}^{LW}$ is calculated using (5), it is possible to determine the other two unknown variables, that is, ${\gamma_S}^+$ and ${\gamma_S}^-$ by inserting ${\gamma_S}^{LW}$ into (7). The values of ${\gamma_S}^+$ and ${\gamma_S}^-$ are then inserted into the following equations to calculate the acid-base components, γ refers to surface energy, A refers to acid and B refers to base, ${\gamma_S}^{AB}$, and the total surface energy, ${\gamma_S}^{Total}$:

$$\begin{aligned} {\gamma_S}^{AB} &= 2\sqrt{({\gamma_S}^+{\gamma_L}^-)}, \\ {\gamma_S}^{Total} &= {\gamma_S}^{LW} + {\gamma_S}^{AB}. \end{aligned} \quad (8)$$

Chen and Chang [20] proposed a semiempirical acid-base approach to understand the interfacial interaction in the CNT thin films, here referred to as Chang-Qin-Chen (CQC) model. In (9), unknowns such as ${P_S}^{LW}$ (the Lifshitz-van der Waals components of the solid) and ${P_s}^a$ and ${P_s}^b$ (principal acid and base values) were determined by multiple regression analysis using a semi-interactive spreadsheet:

$$W_a = \gamma_L(1+\cos\theta) = {P_L}^{LW}{P_S}^{LW} - {P_L}^a{P_S}^b - {P_L}^b{P_S}^a, \quad (9)$$

where the P_L are the liquid components. From the calculated parameters of the solid, that is, ${P_S}^a$ and ${P_S}^b$, the acid-base components, the magnitude of interaction is calculated by the multiplication of ${P_S}^a$ and ${P_S}^b$ which provides a value for the acid-base component of surface energy, ${\gamma_S}^{AB}$, of the CNT thin film using

$${\gamma_S}^{AB} = -{P_S}^a{P_S}^b. \quad (10)$$

The surface is considered as acidic if both ${P_S}^a$ and ${P_S}^b$ are positive, basic when both are negative, and amphoteric if they are opposite in sign.

3. Results and Discussion

3.1. Raman Analysis. Generally, Raman spectroscopy is a helpful technique determining the purity, diameter distribution, and architecture of CNTs. Here, we analysed the Raman spectrum to determine a content of defect site of the MWCNTs. The Raman spectrum of MWCNTs with different treatment (pristine, UV/O_3, and acid) are shown in Figure 1. As can be observed, three kinds of MWCNTs show two characteristic bands: the D-mode (1350 cm^{-1}) and G-mode (1590 cm^{-1}) vibration bands, which correspond to residual ill-organized graphite and tangential C–C stretching vibration [27], respectively. For pristine MWCNTs, the G-band peak is relative stronger compared with those of MWCNTs treated by UV/O_3 and acid, due to low impurities level and structural defect. After UV/O_3 treatment, relative intensity ratio (I_D/I_G) increased from 0.85 to 0.91. In case of acid treatment, the high intensity ratio (1.41) is obtained for the introduction of functional groups such as carbonyl and carboxyl on MWCNT surface. We performed transmission electron microscopy (TEM, JEM-2100F, and JEOL) analysis to confirm whether the surface of the UV/O_3 and acid-treated

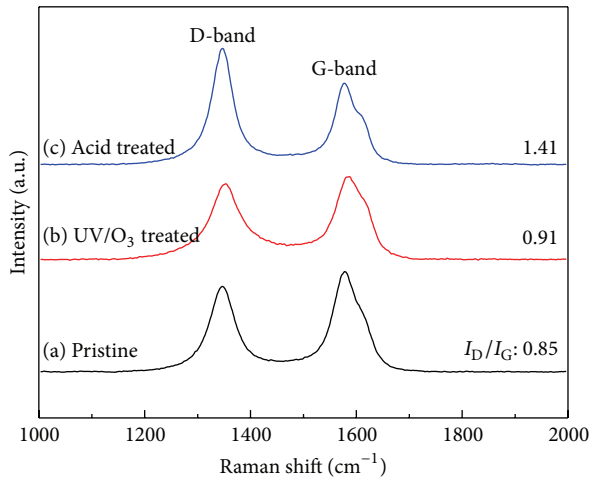

Figure 1: Raman spectrum of MWCNTs with pretreatment under different condition. (a) Pristine, (b) 120 min UV/O_3, and (c) 24-hour acid.

MWCNTs sample is damaged. Figure 2 shows the typical TEM images of MWCNTs with pristine, UV/O_3, and acid treatment. In these images, it was found that UV/O_3 treatment did not cause structural defect on MWCNTs compared with that of acid treatment (yellow circles are defect point), which caused decreasing of properties of MWCNTs.

3.2. Contact Angle Study

3.2.1. UV/O_3- and Acid-Treated MWCNT Thin Films. Effect of UV/O_3- and acid-treated surface modification of MWCNT leads to the formation of functional groups and thus changes the contact angles. It can be seen in Figure 3 that the contact angle (CA) of UV/O_3 modified MWCNT changed after 30 min of treatment for ethylene glycol and glycerol. The contact angle slightly decreased (160–156) after 60 min and significantly decreased (133) at 120 min of UV-treated MWCNT. It initially appeared that 30 min of UV/O_3 treatment induced some extent of hydrophilicity to the MWCNT, as evidenced in the contact angle measured with water, glycerol, and ethylene glycol. This trend is not surprising because the pristine MWCNTs were mainly agglomerated due to a higher surface energy and they started to separate from each other when the cohesive force was reduced due to the UV/O_3 treatment. Similarly, in acid-treated MWCNT thin films, the contact angle decreased, which was significant for 24 hours of treatment no matter what probe liquid was used, as shown in Figure 4.

Figure 5 shows the CA of three different polar solvents on pure PMMA and modified MWCNT-PMMA film. Higher CA was observed for all polar solvents for 30 to 120 min UV/O_3-treated MWCNT/PMMA film samples. However, significantly, decrease in CA for 24-hour acid-treated MWCNT/PMMA sample was clearly observed as shown in Figure 6. It was most likely due to the extended period of treatment which created defects on MWCNT (Figure 2) and resulted in a better interaction between PMMA and MWCNT.

Table 1: Surface energy calculation of treated MWCNT films using Fowkes model.

Sample	γ_S^{tot} (mJ/m^2)	γ_S^{d*} (mJ/m^2)	γ_S^{p*} (mJ/m^2)
Raw CNT	25.00	18.00	7.00
UV/O_3 30 min	44.29	37.00	5.90
UV/O_3 60 min	66.62	59.00	12.00
UV/O_3 120 min	71.43	92.00	13.23
Acid 6 hours	8.01	0.77	7.24
Acid 12 hours	16.88	14.58	3.30
Acid 24 hours	26.73	25.76	0.97

Table 2: Surface energy calculation of treated MWCNT/PMMA nanocomposites using Fowkes model.

Sample	γ_S^{tot} (mJ/m^2)	γ_S^{d*} (mJ/m^2)	γ_S^{p*} (mJ/m^2)
Pure PMMA	12.51	10.14	2.42
UV/O_3 30 min	22.48	20.79	2.19
UV/O_3 60 min	126.86	16.05	11.00
UV/O_3 120 min	145.56	2.75	4.75
Acid 6 hours	13.43	5.30	8.14
Acid 12 hours	20.34	7.66	12.69
Acid 24 hours	26.74	11.54	15.20

3.3. Surface Energy Study

3.3.1. UV/O_3- and Acid-Treated CNT Thin Films. The surface energy calculated from the Fowkes model showed that surface energy values of the 30–120 min UV/O_3-treated thin films were significantly increased with increasing UV/O_3 treatment time (Table 1). The increase of the total surface energy with increasing treatment time was mainly due to increases of both dispersion and acid-base components. From the Gamma$^+$ (electron acceptor) and Gamma$^-$ (electron donor) values reported in Table 1, it can be seen that the surface was predominantly basic and became more basic especially for the 60-minute UV/O_3 treatment. The reason for the predominant basicity is most likely due to the release of hydrogen atoms from some acid groups created on the MWCNT surface as a result of the UV/O_3 treatment. For the acid-treated MWCNT thin films, the total surface energy values were also increased after 6 hours of acid treatment, which is the same as that observed for the UV/O_3-treated MWCNT thin films. The increase of the total surface energy values at 24 hours was mainly due to the increase of the dispersion energy component as there was no improvement of the polar component. However, the increase of the dispersion component was mainly due to very strong acid treatment which may have the potential to break the graphitic structure and leave nonpolar carbon open to the surface.

The surface energy calculated from the Fowkes model for MWCNT-modified PMMA nanocomposites is presented in Table 2. It was observed that all surface energy values of the all UV/O_3-treated MWCNT/PMMA films were significantly improved from 12.51 to 145.56 mJ/m^2. Surface was predominantly basic and became more basic especially for the 60- and 120-minute UV/O_3 treatment. The reason can be attributed

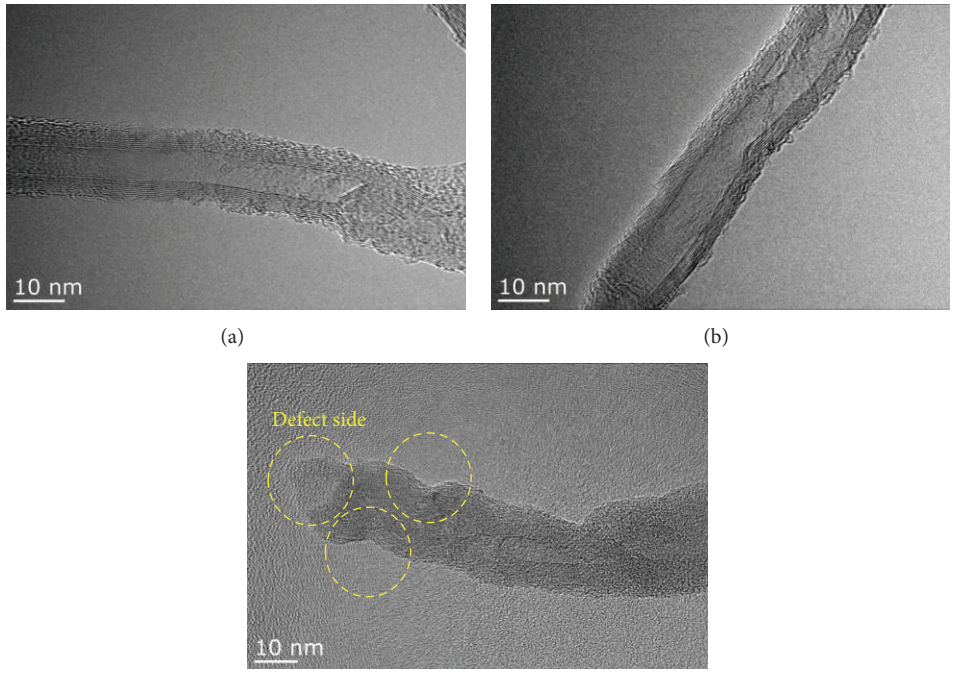

(a) (b) (c)

Figure 2: TEM images of (a) pristine MWCNT, (b) 120 min UV/O_3-treated MWCNT, and (c) 24-hour acid-treated MWCNT.

Table 3: Surface energy calculation of treated MWCNT films using GvOC model.

Sample	γ_S^{tot} (mJ/m^2)	γ_S^{d*} (mJ/m^2)	γ_S^{p*} (mJ/m^2)	γ_S^{+} (mJ/m^2)	γ_S^{-} (mJ/m^2)
Pure PMMA	24.33	18.10	6.12	1.78	5.26
UV/O_3 30 min	44.22	37.70	0.52	0.10	0.65
UV/O_3 60 min	69.51	58.73	10.77	2.83	10.22
UV/O_3 120 min	74.10	91.26	2.84	0.69	2.92
Acid 6 hours	1.19	0.77	0.41	0.008	5.39
Acid 12 hours	6.83	6.59	0.24	0.11	0.13
Acid 24 hours	26.91	26.07	0.84	0.29	0.59

to the release of hydrogen atoms from some acid groups created on the MWCNT surface as a result of the UV/O_3 treatment. For the acid-treated MWCNT/PMMA thin films, the total surface energy values increased after 6 hours of acid treatment and with time of 12 hours and reached very high values for 24 hours of acid treatment. The increase of the total surface energy values at 24 hours was mainly due to the increase of the dispersion energy component as there was no improvement of the polar component. However, the increase of the dispersion component was mainly due to the very strong acid treatment which may have the potential effect on defect structure which was confirmed by TEM images in Figure 2. Calculation of surface energy by using contact angle measurement and fitting to GvOC and CQC model for UV/O_3- and acid-treated film and PMMA nanocomposites are presented in Tables 3, 4, 5, and 6. Exactly the same surface energy increment trend as Fawker model was observed in both models. In addition, CQC model was able to determine the surface nature of MWCNT in thin film or in PMMA nanocomposites. It should be noted that MWCNT film treated by UV/O_3 showed amphoteric surface behaviour; however, acid-treated MWCNT film showed acidic surface characteristics as shown in Table 5. All the PMMA nanocomposites fabricated by UV/O_3 and acid treatment showed amphoteric surface characteristic as shown in Table 6. The results suggest that the wettability changes in thin film or nanocomposites of MWCNT by UV/O_3 or acid treatment due to the change in surface chemistry.

3.4. Electrical Properties of the MWCNT/PMMA Nanocomposites. The electrical properties of the CNT-filled nanocomposites can be regarded as an indicator of the CNTs dispersion in the polymer composite. In our previous study [21], we exquisitely reported the sheet resistance of MWCNT/PMMA nanocomposites containing MWCNTs subjected to various treatments. In the present work, we expanded the scope of the study by introducing sheet resistance data of MWCNT-filled nanocomposites as a function of the treatment time and correlated with the surface energy obtained by measuring contact angle on the CNT-PMMA nanocomposites. Figure 7

Figure 3: Effect of UV/O_3 treatment on contact angle of MWCNT thin film.

shows the scanning electron microscope (SEM) images of the MWCNT/PMMA composite synthesized with pristine MWCNTs and treated by UV/O_3 (120 min) and acid (24 hr). A PMMA sheet exhibited relatively smooth surface compared with that of MWCNT added composites. In case of pristine MWCNT/PMMA composite, CNT was sporadically agglomerated. On the other hand, in case of UV/O_3-treated MWCNT and acid PMMA composites, there was no sign of MWCNT agglomeration due to surface functionalisation. Also, UV/O_3-treated MWCNT/PMMA composite shows the distinguished CNT conducting pathway into the composite. This pathway plays a major role into composite to enhance the electrical conductivity.

Figures 8(a) and 8(b) show the electrical sheet resistance of nanocomposites with MWCNTs treated by UV/O_3 and acid as a function of the treatment time. Figure 8(a) show the decrease of the resistance with increasing the duration of the UV/O_3 treatment. These results indicate that conductive paths in the polymer matrix were formed as a result of enhanced dispersibility due to the UV/O_3 treatment which

Figure 4: Effect of acid treatment on contact angle of MWCNT thin film.

Table 4: Surface energy calculation of treated MWCNT/PMMA nanocomposites using GvOC model.

Sample	γ_S^{tot} (mJ/m^2)	γ_S^{d} (mJ/m^2)	γ_S^{ab} (mJ/m^2)	γ_S^{+} (mJ/m^2)	γ_S^{-} (mJ/m^2)
Raw CNT	11.33	10.15	1.18	1.86	0.19
UV/O_3 30 min	22.72	20.79	1.93	0.45	2.07
UV/O_3 60 min	136.26	116.00	120.26	11.31	77.77
UV/O_3 120 min	146.93	2.75	4.17	0.99	4.39
Acid 6 hours	12.45	5.30	7.15	1.66	7.69
Acid 12 hours	18.80	7.66	11.14	2.68	11.58
Acid 24 hours	24.82	11.54	13.28	3.50	12.59

created functional groups, resulting in a lower resistance than that of the raw MWCNTs in the nanocomposite. Obtained sheet resistance data was compared with surface energy results obtained from various models and concluded that electrical conductivity increases as surface energy of MWCNT increases. On the other hand, in the acid-treated samples (Figure 8(b)), the resistance of the nanocomposite increased with acid treatment time. The results also showed a correlation between surface energy of MWCNT and electrical conductivity. During acid treatment, surface energy of MWCNT was increased as shown in Table 5 and also electrical conductivity reduced (increases in resistance) as shown in Figure 8(b). The decrease in electrical conductivity can be attributed to surface defects while using strong concentration

Figure 5: Effect of UV/O_3 treatment on contact angle of MWCNT/PMMA nanocomposite.

Table 5: Surface energy calculation of treated MWCNT thin films using CQC model.

Sample	γ_S^{tot} (mJ/m^2)	γ_S^{d} (mJ/m^2)	γ_S^{ab} (mJ/m^2)	P_S^{a} (mJ/m^2)$^{1/2}$	P_S^{b} (mJ/m^2)$^{1/2}$	Nature
Raw CNT	19.60	18.04	1.56	3.82	0.41	Amphoteric
UV/O_3 30 min	43.31	3.65	1.34	0.17	2.01	Amphoteric
UV/O_3 60 min	68.09	58.23	9.85	−3.43	2.86	Amphoteric
UV/O_3 120 min	73.96	11.17	2.79	−1.18	2.38	Amphoteric
Acid 6 hours	3.96	0.79	−4.48	−1.05	−4.29	Acidic
Acid 12 hours	13.96	6.53	−2.57	−1.77	−1.45	Acidic
Acid 24 hours	24.01	25.76	−1.75	−2.01	−0.87	Acidic

Figure 6: Effect of acid treatment on contact angle of MWCNT/PMMA nanocomposite.

Table 6: Surface energy calculation of treated MWCNT/PMMA nanocomposites using CQC model.

Sample	γ_S^{tot} (mJ/m^2)	γ_S^{d} (mJ/m^2)	γ_S^{ab} (mJ/m^2)	P_S^{a} (mJ/m^2)$^{1/2}$	P_S^{b} (mJ/m^2)$^{1/2}$	Nature
Pure PMMA	12.46	10.10	2.36	1.06	−2.22	Amphoteric
UV/O_3 30 min	22.58	20.32	2.26	1.08	−2.09	Amphoteric
UV/O_3 60 min	163.12	26.35	9.47	5.02	−3.82	Amphoteric
UV/O_3 120 min	147.16	2.64	4.52	1.50	−3.00	Amphoteric
Acid 6 hours	12.52	5.10	7.41	1.71	−4.32	Amphoteric
Acid 12 hours	19.63	7.36	12.26	2.67	−4.58	Amphoteric
Acid 24 hours	23.11	11.07	12.03	4.47	−2.68	Amphoteric

acid treatment for 6–24 hours [28, 29]. Damaged MWCNT as shown in Figure 2 can reduce or prevent the formation of a conductive pathway in the polymer matrix thus showing the higher resistance. The effect of functional groups available on the CNT surface may also be another reason for this behaviour. Generally, the introduction of functional groups such as oxygen on the CNT surfaces decreases the electrical properties of CNTs, implying that these functional groups disturb the electron flow of individual CNTs into the matrix. Both UV/O_3- and acid-treated MWCNT-PMMA nanocomposites showed a good correlation between calculated surface energy from contact angle measurement and measured sheet resistance. The relationship between surface energy from contact angle measurement and electrical conductivity has not been reported yet.

4. Conclusions

The dispersibility of pristine and functionalized MWCNT was characterized using contact angle measurements and then fitted with various models for surface energy measurement. The surface energy measured from the contact angle

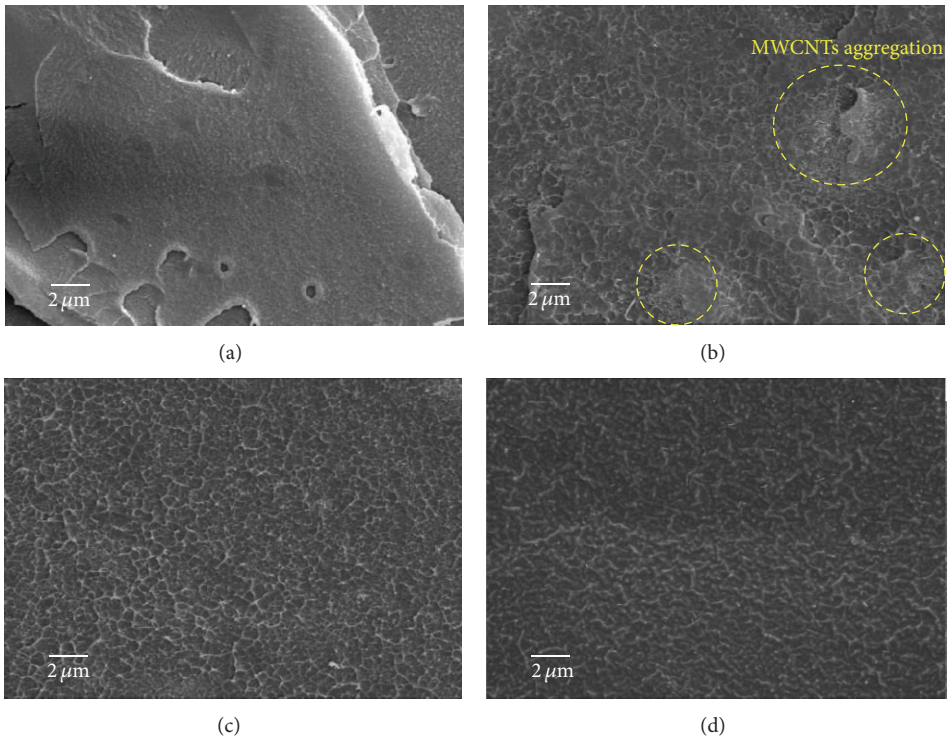

FIGURE 7: SEM images of (a) PMMA, (b) pristine MWCNT/PMMA, (c) 120 min UV/O_3 MWCNT/PMMA, and (d) 24-hour acid-treated MWCNT/PMMA composite.

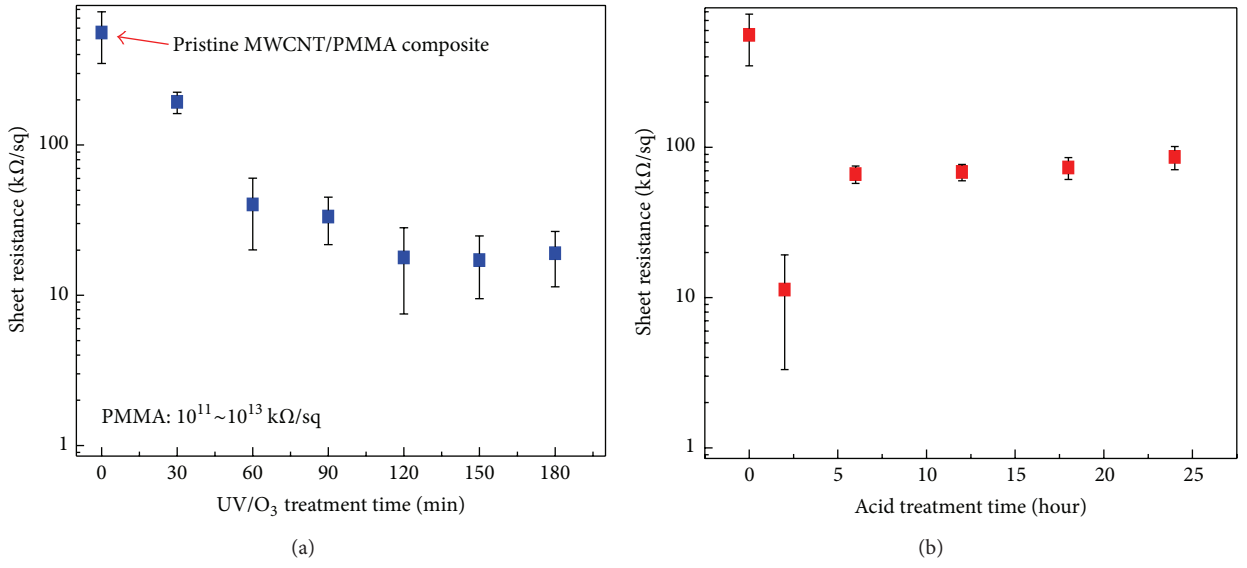

FIGURE 8: Sheet resistance of MWCNT/PMMA composite with MWCNTs pretreated by (a) UV/O_3 and (b) acid.

values also elucidated the internal mechanism of dispersion and CNT surface functionality. We also demonstrated the successful functionalization of MWCNT by acid and UV/O_3 treatments. It can be concluded that both treatments resulted in better dispersion of the MWCNTs into the various liquid and PMMA nanocomposites. Moreover, it was found that the surface energy of the MWCNT/PMMA nanocomposite was directly related to conductive paths into the nanocomposite by utilizing a concept of the electrical properties including the oxygen content of the MWCNT surface. This work will be helpful in understanding and estimating the conditions suitable for dispersing MWCNT in a polymer matrix to yield nanocomposites with desirable properties and not using expensive XPS studies for clarification. Furthermore, it can be an investigative tool of MWCNT-filled nanocomposites used in electronics or microfluidic applications.

Conflict of Interests

The authors declare that there is no conflict of interests regarding the publication of this paper.

Acknowledgments

This work was supported by the Industrial Strategic Technology Development Program (10045177, Development of Resistive Ceramic Thin Film using Solution Process and Low Temperature Thin Film Vacuum Getter) and the Human Resources Development Program (no. 20124030200130) of the Korea Institute of Energy Technology Evaluation and Planning (KETEP) grant funded by the Korea government Ministry of Trade, Industry and Energy.

References

[1] J.-M. Park, D.-S. Kim, J.-R. Lee, and T.-W. Kim, "Nondestructive damage sensitivity and reinforcing effect of carbon nanotube/epoxy composites using electro-micromechanical technique," *Materials Science and Engineering C*, vol. 23, no. 6–8, pp. 971–975, 2003.

[2] J. Zhu, J. Kim, H. Peng, J. L. Margrave, V. N. Khabashesku, and E. V. Barrera, "Improving the dispersion and integration of single-walled carbon nanotubes in epoxy composites through functionalization," *Nano Letters*, vol. 3, no. 8, pp. 1107–1113, 2003.

[3] T. M. Long, S. Prakash, M. A. Shannon, and J. S. Moore, "Water-vapor plasma-based surface activation for trichlorosilane modification of PMMA," *Langmuir*, vol. 22, no. 9, pp. 4104–4109, 2006.

[4] H.-C. Lee, M. S. Akhtar, J. G. Park, K.-J. Kim, S.-K. Lee, and O.-B. Yang, "Carbon nanotube (CNT)-polymethyl methacrylate (PMMA) composite electrolyte for solid-state dye sensitized solar cells," *Journal of Nanoscience and Nanotechnology*, vol. 10, no. 5, pp. 3502–3507, 2010.

[5] L. M. Clayton, A. K. Sikder, A. Kumar et al., "Transparent poly(methyl methacrylate)/single-walled carbon nanotube (PMMA/SWNT) composite films with increased dielectric constants," *Advanced Functional Materials*, vol. 15, no. 1, pp. 101–106, 2005.

[6] R. Ou, S. Gupta, C. A. Parker, and R. A. Gerhardt, "Fabrication and electrical conductivity of Poly(methyl methacrylate) (PMMA)/carbon black (CB) composites: comparison between an ordered carbon black nanowire-like segregated structure and a randomly dispersed carbon black nanostructure," *The Journal of Physical Chemistry B*, vol. 110, no. 45, pp. 22365–22373, 2006.

[7] L. Li, E. Liu, L. Z. Goh, and Y. P. Lee, "Comparison between poly(methyl methacrylate)-carbon black and polyaniline conductive coatings," *Journal of Nanoscience and Nanotechnology*, vol. 8, no. 5, pp. 2637–2642, 2008.

[8] M. A. Aldosari, A. A. Othman, and E. H. Alsharaeh, "Synthesis and characterization of the in situ bulk polymerization of PMMA containing graphene sheets using microwave irradiation," *Molecules*, vol. 18, no. 3, pp. 3152–3167, 2013.

[9] X. Y. Yuan, L. L. Zou, C. C. Liao, and J. W. Dai, "Improved properties of chemically modified graphene/poly(methyl methacrylate) nanocomposites via a facile in-situ bulk polymerization," *Express Polymer Letters*, vol. 6, no. 10, pp. 847–858, 2012.

[10] R. Andrews and M. C. Weisenberger, "Carbon nanotube polymer composites," *Current Opinion in Solid State and Materials Science*, vol. 8, no. 1, pp. 31–37, 2004.

[11] B. Philip, J. K. Abraham, A. Chandrasekhar, and V. K. Varadan, "Carbon nanotube/PMMA composite thin films for gas-sensing applications," *Smart Materials and Structures*, vol. 12, no. 6, pp. 935–939, 2003.

[12] J. K. Abraham, B. Philip, A. Witchurch, V. K. Varadan, and C. Channa Reddy, "A compact wireless gas sensor using a carbon nanotube/PMMA thin film chemiresistor," *Smart Materials and Structures*, vol. 13, no. 5, pp. 1045–1049, 2004.

[13] N. Karousis, N. Tagmatarchis, and D. Tasis, "Current progress on the chemical modification of carbon nanotubes," *Chemical Reviews*, vol. 110, no. 9, pp. 5366–5397, 2010.

[14] F. Lu, L. Gu, M. J. Meziani et al., "Advances in bioapplications of carbon nanotubes," *Advanced Materials*, vol. 21, no. 2, pp. 139–152, 2009.

[15] P. Garg, B. P. Singh, G. Kumar et al., "Effect of dispersion conditions on the mechanical properties of multi-walled carbon nanotubes based epoxy resin composites," *Journal of Polymer Research*, vol. 18, no. 6, pp. 1397–1407, 2011.

[16] P.-C. Ma, N. A. Siddiqui, G. Marom, and J.-K. Kim, "Dispersion and functionalization of carbon nanotubes for polymer-based nanocomposites: a review," *Composites Part A: Applied Science and Manufacturing*, vol. 41, no. 10, pp. 1345–1367, 2010.

[17] R. J. Good, *Contact Angle, Wettability and Adhesion*, edited by K. L. Mittal, VSP, Utrecht, The Netherlands, 1993.

[18] A. A. Kafi, K. Magniez, and B. L. Fox, "Measuring the adhesion force on natural fibre surface using scanning probe microscopy," *Journal of Adhesion Science and Technology*, vol. 26, no. 1–3, pp. 175–187, 2012.

[19] C. J. van Oss, M. K. Chaudhury, and R. J. Good, "Monopolar surfaces," *Advances in Colloid and Interface Science*, vol. 28, pp. 35–64, 1987.

[20] F. Chen and W. V. Chang, "Applicability study of a new acid-base interaction model in polypeptides and polyamides," *Langmuir*, vol. 7, no. 10, pp. 2401–2404, 1991.

[21] S. Kim, Y.-I. Lee, D.-H. Kim et al., "Estimation of dispersion stability of UV/ozone treated multi-walled carbon nanotubes and their electrical properties," *Carbon*, vol. 51, no. 1, pp. 346–354, 2013.

[22] F. M. Fowkes, "Determination of interfacial tensions, contact angles, and dispersion forces in surfaces by assuming additivity of intermolecular interactions in surfaces," *Journal of Physical Chemistry*, vol. 66, no. 2, p. 382, 1962.

[23] F. M. Fowkes, "Additivity of intermolecular forces at interfaces. I. Determination of the contribution to surface and interfacial tensions of dispersion forces in various liquids," *The Journal of Physical Chemistry*, vol. 67, no. 12, pp. 2538–2541, 1963.

[24] D. K. Owens and R. C. Wendt, "Estimation of the surface free energy of polymers," *The Journal of Physical Chemistry A*, vol. 13, no. 8, pp. 1741–1747, 1969.

[25] P. C. Hiemenz and R. Rajagopalan, *Principles of Colloid and Surface Chemistry*, Taylor & Francis, 3rd edition, 1997.

[26] C. J. van Oss, M. K. Chaudhury, and R. J. Good, "Monopolar surfaces," *Advances in Colloid and Interface Science*, vol. 28, pp. 35–64, 1987.

[27] N. Pierard, A. Fonseca, J.-F. Colomer et al., "Ball milling effect on the structure of single-wall carbon nanotubes," *Carbon*, vol. 42, no. 8-9, pp. 1691–1697, 2004.

[28] S.-M. Yuen, C.-C. M. Ma, C.-L. Chiang, and C.-C. Teng, "Morphology and properties of aminosilane grafted MWCNT/polyimide nanocomposites," *Journal of Nanomaterials*, vol. 2008, Article ID 786405, 15 pages, 2008.

[29] N. R. Rajendran Royan, A. B. Sulong, J. Sahari, and H. Suherman, "Effect of acid- and ultraviolet/ozonolysis-treated MWCNTs on the electrical and mechanical properties of epoxy nanocomposites as bipolar plate applications," *Journal of Nanomaterials*, vol. 2013, Article ID 717459, 8 pages, 2013.